An Analysis of Coupling between the x_1 and x_{12} Interferometers for LISA Pathfinder

Brittany Howard

August 8, 2016

Abstract

For an unknown reason, noise from the jittering of the spacecraft housing LISA Pathfinder (LPF) is appearing in the differential measurement between its two test masses (TM's). This phenomenon manifests as a small but measurable coupling between the readouts of LPF's two heterodyne interferometers, x_1 and x_{12}. In this study, two LISA Pathfinder experiments are analyzed using three methods in an effort to characterize and quantify the coupling and potentially identify its source. The main question considered is this: does the coupling change with the absolute displacement between the TM's? As a result of this work, reliable values for coupling between LPFr's x_1 and x_{12} interferometers are found, and they are seen to depend on the absolute displacement between the test masses to some degree.

1 Introduction

1.1 LISA Pathfinder

LISA Pathfinder (LPF) is a European Space Agency satellite which serves as a technology demonstrator for LISA, planned to be the first space-based gravitational wave detector. LPF utilizes key LISA technologies including picometer-precision metrology, microNewton thrusters, and the control of a drag-free test mass in such a way that it is influenced solely by the geodesics of local spacetime [2].

While LISA will consist of three satellites in a triangular configuration creating interferometer armlengths on the order of millions of kilometers, LPF is a single satellite with a much shorter armlength of 376.00 ± 0.05 mm between its two test masses [1]. This provides a simpler, relatively inexpensive way to test LISA's technology before investing the necessary time and money into the full LISA mission.

LISA Pathfinder's importance lies in the fact that it represents the first time humanity has had access to an interferometer in space. LISA will be a large investment, and it requires a great deal of testing in preparation for launch,

which is where LPF comes in. While a replica of LPF's optical bench has been built on Earth and thoroughly characterized, being in space mitigates or reduces many of the earthly noise source such as seismic activity, while introducing some new ones like the vibrations of the satellite due to its thrusters. In order to make LISA as precise an instrument as possible, it is necessary to conduct a variety of experiments with LPF in order to understand the types of noise we can expect LISA to experience as completely as possible.

LISA Pathfinder has been a highly successful mission thus far. With LPF, the scientific community has demonstrated the ability to place the test masses in sub-femto-g freefall with a noise level five times lower than the threshold required for the mission [1].

1.2 Optical Metrology System

Onboard the satellite is a system of highly precise interferometers, called the Optical Metrology System (OMS), which monitors the changes in position and angles between the two test masses and the satellite itself. The values read out by the OMS are as follows [2]:

- x_1: The displacement of test mass 1 relative to the spacecraft
- x_{12}: The displacement of test mass 2 relative to test mass 1
- η_1 and ϕ_1: The angular fluctuations of test mass 1
- η_2 and ϕ_2: The angular fluctuations of test mass 2

For a diagram showing the orientation of the LPF system, see figure 1.

1.3 LISA Pathfinder Experiments

LISA Patfinder's operations are broken down into many individual experiments, each of which is meant to test a specific aspect of the satellite's performance. For this analysis, two experiments were analyzed using the same methods so as to get as complete a picture as possible of how the coupling between x_1 and x_{12} varies as a function of distance between the test masses. Each of the experiments analyzed will be briefly introduced below.

1.3.1 Armlength-Mismatch Experiment

Beginning at the nominal zero position, the test masses underwent a large slew, separating by 10 micrometers (9 wavelengths). This created long stretches of data at two distanct x_{12} positions, allowing many datapoints to be made and averaged. In turn, this created very reliable measurements for coupling at two x_{12} positions.

For a descriptive image of the armlength-mismatch experiment, see figure 2.

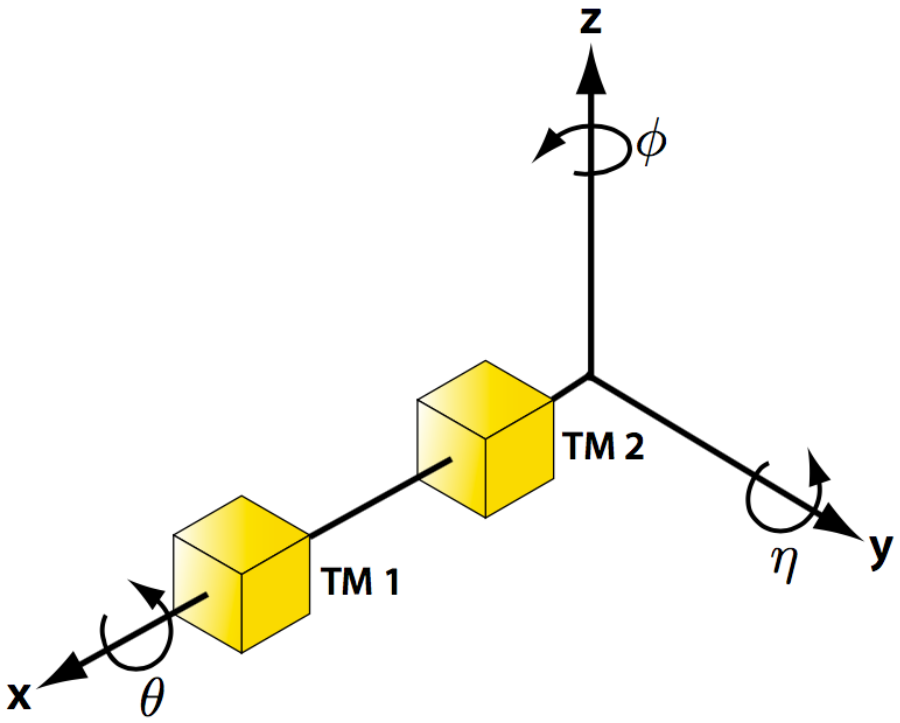

Figure 1: A digram defining the axes for the angular and longitudinal measurements of the test masses by LISA Pathfinder's OMS [3].

1.3.2 x_1 Injection Experiment

This was a quick, dedicated experiment for measuring the coupling between x_1 and x_{12}. A 400 mHz signal was injected into x_1, creating an opportunity to observe how much of the signal leaked into x_{12}. While it only allowed the coupling to be measured at one x_{12} position, this experiment was useful because the exact frequency at which to look for the signal in x_{12} (400 mHz) is known.

For a descriptive image of the x_1 injection experiment, see figure 3.

2 Motivation

The idea of this investigation is to determine to what degree x_1 (the displacement of test mass 1 from the spacecraft) is coupled to x_{12} (the displacement of test mass 2 from test mass 1). Understanding how the coupling changes with the distance between test masses gives some insight into how the noise from spacecraft vibrations affects the overall system. Ultimately, this is a useful endeavor because if noise sources are well-characterized, their effects can be

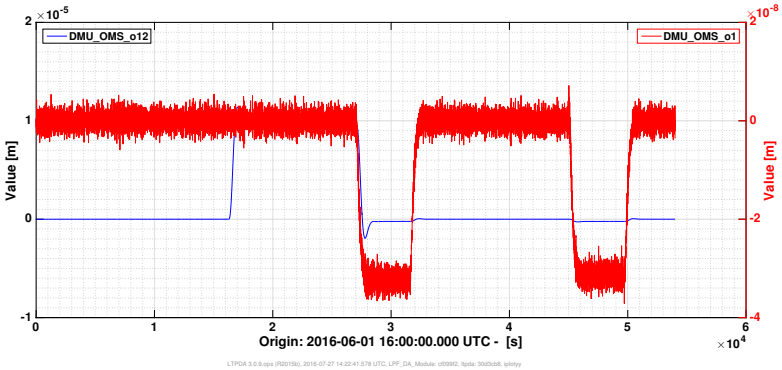

Figure 2: A plot showing x_1 and x_{12} as a function of time for the x_1 injection experiment. x_1 is in red, and x_{12} is in blue.

subtracted from the output of the OMS. This, in turn, will make LISA a more precise gravitational wave detector.

See figure 4 for a diagram of the geometry involved in the system being analyzed. The idea is that as the test masses move relative to each other and the optical bench in between them, the angle of incidence of the lasers on their photodiodes remains constant. However, the center of the beam will move laterally across the photodiodes' surfaces.

This is important because the photodiodes are each divided into four quadrants, and the amount of light measured on each quadrant is recorded. Ideally, if the beams were perfectly centered, the amount of light falling onto each quadrant of a photodiode would be the same, and so the OMS would consider the light beam to come in at a right angle. However, due to the fact that the laser beams move laterally across the photodiodes' surface, the angle may not change in reality as the test masses move along the axis between them, but the OMS would "think" it does. This may cause coupling between x_1 and x_{12}.

3 Methods of Analysis

Three methods of solving for the coupling were used, which will be called the transfer function (TFE) method, the discrete transfer function (DTFE) method, and the debumping method. The debumping method's algorithm was already written when this project was begun, but it is necessary to the other two methods, so it will be briefly described in its own subsection.

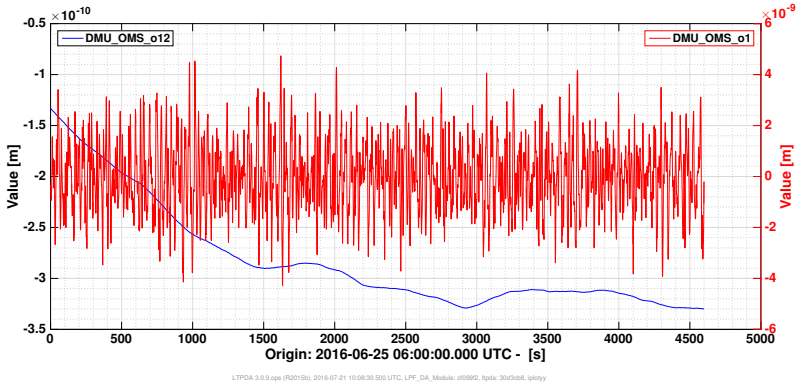

Figure 3: A plot showing x_1 and x_{12} as a function of time for the x_1 injection experiment. x_1 is in red, and x_{12} is in blue.

3.1 Debumping Method

The debumping method consists of PSD minimisation through linear combination of other degrees-of-freedom. It is sophisticated, but gives a non-unique solution for the coupling. A more precise method was needed, hence this project to develop the following two methods.

3.2 Discrete Transfer Function Estimate (DTFE) Method

The discrete transfer function estimate method is carried out identically to the transfer function estimate method, which will be described in section 3.3, with a single difference; rather than a generic transfer function, a discrete transfer function is used. This is possible when one already knows at which frequency or frequencies to search for coupling. In this study, the DTFE method was used on the x_1 injection experiment; because the experiment involved injecting a signal of a known frequency (400 mHz), it was possible to use a discrete transfer function that looks only at the frequency in question. This eliminates noise entering the measurement from other frequencies at which coupling is not expected anyway and increases the overall precision of the method.

3.3 Transfer Function Estimate (TFE) Method

First, the data from the relevant experiment was downloaded from the LPF database and preprocessed. During the preprocessing, all data is shortened to match the length of the input piece of data. Additionally, all pieces of data are set to begin and end at the same points in time and are resampled at the same rate.

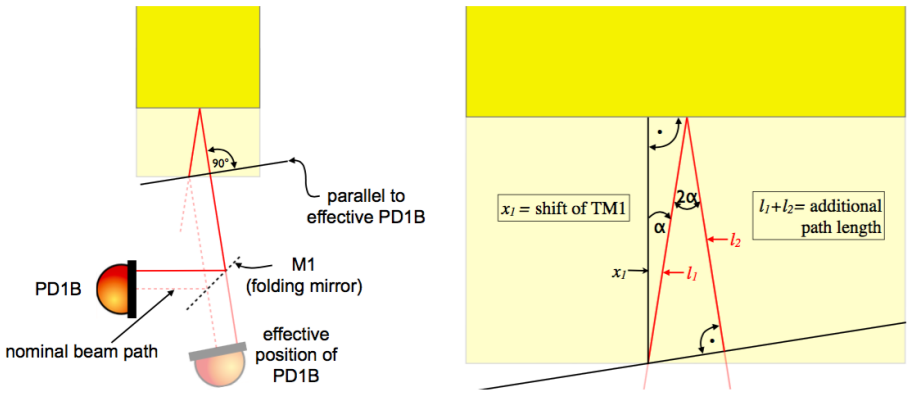

Figure 4: A sketch of the geometry relevant to calculating the coupling [4].

After this setup was finished, x_1 and x_{12} were plotted as a function of time so that one or more sections of transient-free data could be selected. Then these subsets were split from the rest of the data, as shown in Figure 5. From this point on, only these sections of the data were analyzed.

From there, each of the data segments being considered was further sliced into individual segments of about 100 seconds each. This was an ideal length of time because it was just long enough to allow the measurement of signals at the lowest frequencies we expected coupling between the x_1 and x_{12} interferometers, while being short enough to allow many small segments to be made from each data set. This was desirable because the more small segments available, the more data points with which to populate the final plot and estimate how the coupling between x_1 and x_{12} changes as a function of the distance between the two test masses.

The next step in the method is to correct Δg, which is a quantity defined as follows:

$$\Delta g(t) = \Delta\ddot{x}(t) + \omega_2^2 \Delta x(t) + \Delta\omega_{12}^2 x_1(t) - g_c(t) - g_\Omega(t) \tag{1}$$

where $\Delta\ddot{x}(t)$ is the numerical second time derivative of $\Delta x(t)$, g_c is the control force, $g_\Omega(t)$ is the centrifugal correction, and $\Delta\omega_{12}$ is the differential stiffness, defined as $\Delta\omega_{12} = \omega_2^2 - \omega_1^2$ [1].

Δg is the change in the testmasses' acceleration, and it is the primary observable with which gravitational waves will be detected in the full LISA mission.

To correct Δg for a given segment of data, the debumping algorithm is run on the the data, and then the p_y, p_z, and p_η parameters output are recorded into the transfer function method script. Then, using the expression for Δg given in equation 1, a new value is calculated by multiplying each term in the equation by its corresponding parameter from the debumping algorithm. In effect, a new

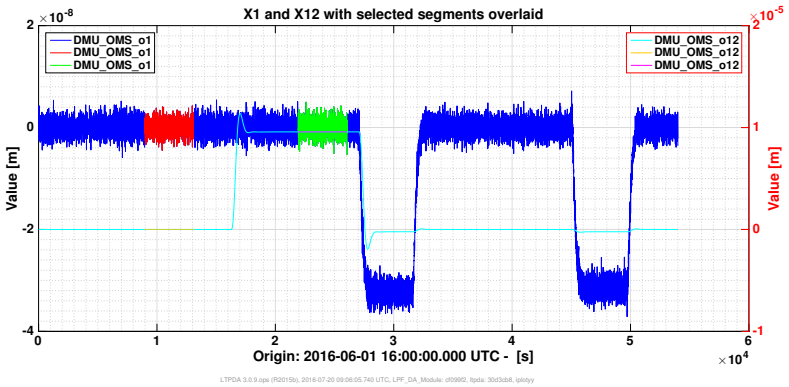

Figure 5: A plot of x_1 and x_{12} as a function of time for the armlength-mismatch experiment. x_{12} is in cyan, and x_1 is in blue. The differently-colored sections represents the two data segments chosen to be analyzed for this experiment. Each of these sections was further broken up into 41 smaller segments of about 100 seconds each.

formula for the average $\Delta g_{corrected}$ for a given data segment is defined as:

$$\overline{\Delta g}_{corrected} = \ddot{x}_{12} - p_\eta \ddot{\bar{\eta}} - p_z \ddot{\bar{z}} - p_y \ddot{\bar{y}} \tag{2}$$

where:

- $\Delta \ddot{\bar{x}}_{12}$ is the change in the numerical second time derivative of x_{12}.
- p_η, p_z, and p_y are parameters obtained from the debumping algorithm.
- $\ddot{\bar{\eta}}$ is defined as the second numerical time derivative of $\frac{\eta_1+\eta_2}{2}$. η_1 and η_2 are angular values read in from LPF's OMS for each of the test masses.
- $\ddot{\bar{z}}$ is defined as the second numerical time derivative of $\frac{z_1+z_2}{2}$. z_1 and z_2 are displacement values read in from LPF's OMS for each of the test masses.
- $\ddot{\bar{y}}$ is defined as the second numerical time derivative of $\frac{y_1+y_2}{2}$. y_1 and y_2 are displacement values read in from LPF's OMS for each of the test masses.

The next step in the process was to calculate the average coherence between $\ddot{x}_1$ and $\Delta g_{corrected}$ for each small data segment. For an example of the coherence as a function of frequency for one small segment in the armlength-mismatch experiment, see Figure 6.

In signal processing, coherence is a statistic that indicates to what extent one signal may be predicted by another. For example, given two signals, A(t) and B(t), the coherence between A and B will be a real-valued number that suggests how much the signal A affects the signal B. For LISA Pathfinder experiments,

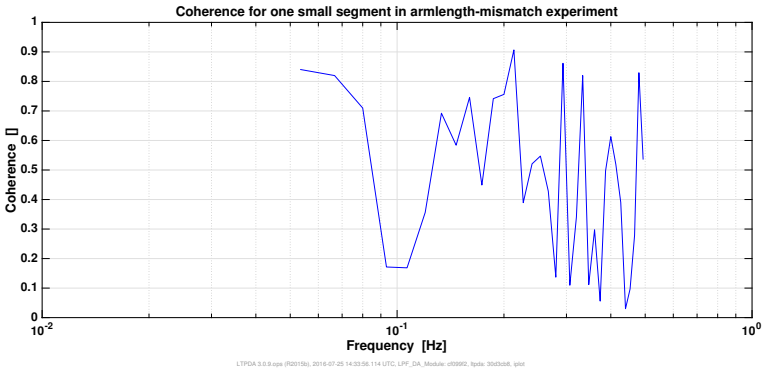

Figure 6: A plot of the coherence between $\ddot{x}_1$ and $\Delta g_{corrected}$ as a function of frequency for one small segment in the armlength-mismatch experiment. The average of the coherence over this range is taken in order to determine whether it is worth continuing to analyze this particular small segment in search of coupling between x_1 and x_{12}.

the coherence is usually between 0 and 1. If the coherence between two signals is 0, that means they are completely unrelated.

Because there was so much data, it was beneficial to calculate coherence for each small segment and then discard the ones with coherence below a certain threshold. This was a reasonable thing to do because if a segment had low coherence, it would also show little to no coupling between x_1 and x_{12} and was therefore not interesting for the analysis. This allowed a significant speed-up to the code's runtime, which was important because the analysis was heavy and took a rather long time to run through all of the input data.

After the low-coherence segments were discarded from the analysis, the transfer function from $\Delta g_{corrected}$ to $\ddot{x}_1$ was calculated for each remaining segment.

Next, transfer function values were plotted as a function of frequency, as shown in Figure 7. Looking at the amplitude component of the transfer functions, a range of frequencies yielding a relatively flat area of transfer function values was selected. The specific values were the range between 95 and 240 mHz.

Next, the mean transfer function value for each small data segment within the selected frequency range was taken. This value was the final product, the mean coupling between x_1 and x_{12} for each small segment. For a plot showing the range of coupling values obtained for the armlength-mismatch experiment, see figure 8.

This entire process is referred to as the "transfer function method", and it was applied to several LPF experiments along with the debumping method.

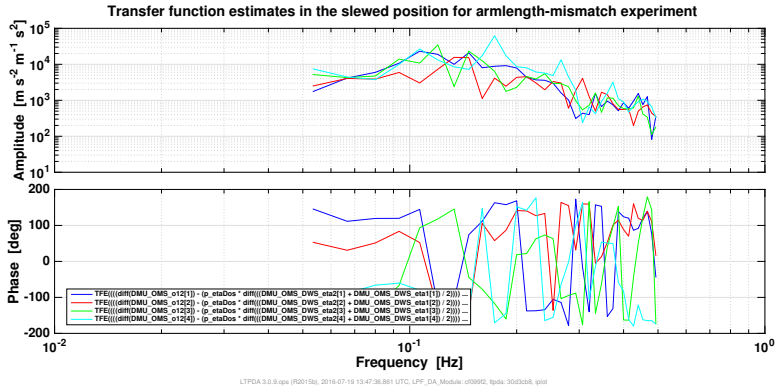

Figure 7: A plot of transfer function value as a function of frequency for a few small segments in the slewed position of the armlength-mismatch experiment. Transfer functions give complex numbers when evaluated; the real component corresponds to the amplitude, and the imaginary component corresponds to the phase. For this analysis method, we are interested only in the amplitude, which is displayed in the top subplot. Note the relatively smooth area in the frequency range from 95-240 mHz.

4 Results

The final results are listed in table 1 and displayed in figure 9. The mean coupling is calculated at each position of x_1 for each experiment using each method. While there is a noticeable spread in the values calculated, it can be inferred that they are all fairly accurate due to the fact that all of the measurements, despite coming from different experiments and different measurements, yield coupling results with the same order of magnitude. Additionally, studies completely before this one (using different methods and different experiments) gave preliminary coupling results for x_1 and x_{12} in LPF to have a mean of -1.895×10^{-5}. This lends additional credence to these new values' accuracy.

5 Future Work

A dedicated LPF experiment would allow the affects of test mass distance on the coupling to be analyzed more completely. Therefore, I propose conducting an experiment as follows: Starting with the test masses relatively close together at a distance of 9 wavelengths (about 10 micrometers) inward from the nominal position, inject a 400 mHz signal into x_1. Then move the test masses slightly farther apart, one wavelength away, and repeat the injection. Continue this process until the test masses are a distance of 9 wavelengths past their nominal position.

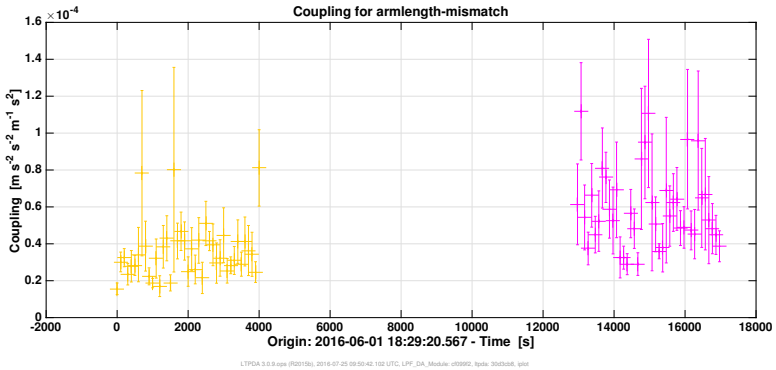

Figure 8: A plot showing coupling values from x_1 to x_{12} with respect to time for the armlength-mismatch experiment. These are results from the TFE method. In yellow are datapoints from the nominal x_{12} position, and in magenta are datapoints from the slewed position. In figure 9, these two groups are averaged to become one datapoint each.

Table 1: The mean couplings that were calculated between x_1 and x_{12}, organized by x_1 position, experiment, and analysis method.

x_1 position	Experiment	Method	Mean Coupling	Error
Nominal	Armlength-mismatch	TFE	4.447E-05	2.670E-06
Nominal	Armlength-mismatch	Debumping	2.416E-05	3.933E-07
Nominal	x_1 injection	TFE	4.962E-05	2.669E-06
Nominal	x_1 injection	Debumping	-1.877E-05	1.232E-06
Nominal	x_1 injection	DTFE	-1.021E-05	1.286e-06
Slewed (∼10 micrometers)	Armlength-mismatch	TFE	7.26E-05	3.857E-06
Slewed (∼10 micrometers)	Armlength-mismatch	Debumping	1.646E-05	6.307E-07

Analysis could then be performed using the DTFE method as described in this paper, checking to see how much of the 400 mHz injection leaks from x_1 into x_{12} at each step in the experiment. This would produce datapoints along the entire possible range of x_{12} and allow the plot shown in figure 9 to be populated much more thoroughly. This experiment would also create the potential to find a value of x_{12} for which the coupling is minimized, hence minimizing the system's error.

6 Final Observations

Coupling **does** appear to change with x_{12} displacement to some degree. This means that as the absolute distance between TM's changes, so does the extent

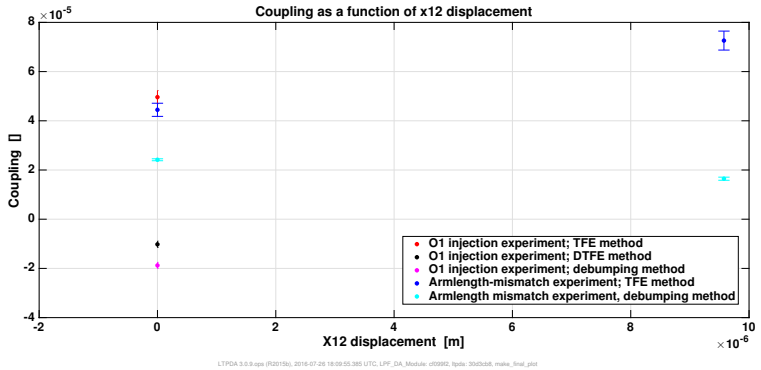

Figure 9: The final plot of this analysis's results. Coupling (unit-less) is along the y-axis with x_{12} displacement in meters along the x-axis. Each combination of experiment and analysis method is given its own marker color.

to which the spacecraft's jittering affects the differential measurement between TM's.

However, the TFE, DTFE, and debumping methods show different trends as to how this relationship varies. While the reason for this discrepancy is not exactly clear, it is important to consider which analysis method is likely to give the most accurate results. As mentioned in section 3.1, debumping is sophisticated but gives non-unique results. Therefore, it should be considered the least trustworthy of the three methods.

The DTFE method, on the other hand, should be considered the most trustworthy; as mentioned in section 3.2, it is usable only when one already knows at which frequency or frequencies coupling may be found. Therefore, there is less noise in the measurement.

The TFE method from section 3.3 is a good middle-ground. Although it is less reliable than the DTFE method, it can be used without knowing which frequencies to search for coupling and is still significantly more precise than debumping.

7 Acknowledgements

I would like to thank the following people and institutions for their aid in this work:

- University of Florida
- Albert Einstein Institute for Gravitational Wave Physics, Hannover
- National Science Foundation

- Dr. Martin Hewitson
- Dr. Guido Mller
- Sarah Paczkowksi
- The LISA Pathfinder Team

References

[1] M. Armano, H. Audley, G. Auger, J. T. Baird, M. Bassan, P. Binetruy, M. Born, D. Bortoluzzi, N. Brandt, M. Caleno, L. Carbone, A. Cavalleri, A. Cesarini, G. Ciani, G. Congedo, A. M. Cruise, K. Danzmann, M. de Deus Silva, R. De Rosa, M. Diaz-Aguiló, L. Di Fiore, I. Diepholz, G. Dixon, R. Dolesi, N. Dunbar, L. Ferraioli, V. Ferroni, W. Fichter, E. D. Fitzsimons, R. Flatscher, M. Freschi, A. F. García Marín, C. García Marirrodriga, R. Gerndt, L. Gesa, F. Gibert, D. Giardini, R. Giusteri, F. Guzmán, A. Grado, C. Grimani, A. Grynagier, J. Grzymisch, I. Harrison, G. Heinzel, M. Hewitson, D. Hollington, D. Hoyland, M. Hueller, H. Inchauspé, O. Jennrich, P. Jetzer, U. Johann, B. Johlander, N. Karnesis, B. Kaune, N. Korsakova, C. J. Killow, J. A. Lobo, I. Lloro, L. Liu, J. P. López-Zaragoza, R. Maarschalkerweerd, D. Mance, V. Martín, L. Martin-Polo, J. Martino, F. Martin-Porqueras, S. Madden, I. Mateos, P. W. McNamara, J. Mendes, L. Mendes, A. Monsky, D. Nicolodi, M. Nofrarias, S. Paczkowski, M. Perreur-Lloyd, A. Petiteau, P. Pivato, E. Plagnol, P. Prat, U. Ragnit, B. Raïs, J. Ramos-Castro, J. Reiche, D. I. Robertson, H. Rozemeijer, F. Rivas, G. Russano, J. Sanjuán, P. Sarra, A. Schleicher, D. Shaul, J. Slutsky, C. F. Sopuerta, R. Stanga, F. Steier, T. Sumner, D. Texier, J. I. Thorpe, C. Trenkel, M. Tröbs, H. B. Tu, D. Vetrugno, S. Vitale, V. Wand, G. Wanner, H. Ward, C. Warren, P. J. Wass, D. Wealthy, W. J. Weber, L. Wissel, A. Wittchen, A. Zambotti, C. Zanoni, T. Ziegler, and P. Zweifel. Sub-femto-g free fall for space-based gravitational wave observatories: Lisa pathfinder results. *Phys. Rev. Lett.*, 116:231101, Jun 2016.

[2] Heather E Audley. *Preparing for LISA Pathfinder Operations: Characterisation of the Optical Metrology System.* PhD thesis, 2014.

[3] N. Gradmann R. Wegener, R. Gerndt and D. Kolbe. Ltp user manual. technical report s2-asd-ma-3004 ltp. *ASD*, 2014.

[4] Gudrun Wanner. *Complex optical systems in space: numerical modelling of the heterodyne interferometery of LISA Pathfinder and LISA.* PhD thesis, Laser Interferometry & Gravitational Wave Astronomy, AEI-Hannover, MPI for Gravitational Physics, Max Planck Society, 2010.